

Modelling Tidal Flow in Great Bay, NH: Adding the Frictional Effects of Eelgrass to the ADAM Model

Safak N. Ertürk

Istanbul Teknik Üniversitesi,
Geminaatve Deniz Bilimleri Fakültesi
Ayazaa, 80626 Istanbul, TURKEY
Phn: +90 (212) 285 6382
safak@sariyer.cc.itu.edu.tr

Frederick T. Short

University of New Hampshire,
Jackson Estuarine Laboratory
Durham, NH 03824, USA
Phn: (603) 862 2175
Fax: (603) 862 1101
Fred.Short@unh.edu

August 03, 2002

Keywords: Eelgrass, bottom friction, tidal flats, flooding and dewatering, nonlinear kinematic model, M_2 tide, USA, New Hampshire, Great Bay Estuary.

Abstract

Tidal flow in Great Bay, New Hampshire, has been simulated by using a finite element numerical model as described in Ip *et al.* (1998). The model is a two-dimensional, nonlinear, time stepping model, which incorporates two-dimensional wave physics with a porous medium underlying the sediment surface to simulate flooding and draining processes on tidal flats. The model is calibrated for the M_2 tidal forcing by adjusting the bottom friction coefficient. The accuracy of the simulation results is demonstrated by comparison with the tidal elevations and cross-section averaged currents reference data from 1975 Great Bay field study (Swift and Brown, 1983). The frictional effects of eelgrass distribution on the tidal flow are explored. Eelgrass beds are treated as extra dampers and the bottom friction coefficient values are modified to reflect the eelgrass distribution in 1990. Addition of eelgrass to the model altered the velocity values both within the eelgrass beds and in the channels and increased the water surface area at mean low water.

Introduction

Tidal currents and surface elevation changes dominate the physics of shallow estuaries. In cases where tidal range is similar to the mean depth, the physics is non-linear. As the offshore tide propagates into an estuary, it becomes distorted because of non-linear processes. The interaction between estuarine geomorphology and tidal forcing produces asymmetries between flood and ebb currents (Pritchard, 1955). Prediction of the flow field is difficult in estuaries due to these distortions introduced by hydrodynamic non-linearities. Kreiss (1957) observed the asymmetry between flood and ebb currents in tidal rivers. He found that the flood current is stronger in speed but shorter in duration than the ebb flow.

The primary force balance is between friction and the pressure gradient in most shallow tidal embayments (Friedrichs *et al.*, 1992). Swift and Brown (1983) verified this balance observationally throughout the Great Bay Estuary. Friction can have a major influence on the tide, primarily because of the low frequencies (and thus long wave lengths) involved. Frictional effects increase with: decreased depth, increased tidal amplitude, or decreased frequency of the various frequency elements that compose the tidal signal (tidal constituents). The major impact of linear friction on a tidal wave is to reduce its amplitude, shorten its wavelength, and slow it down. Higher frequency tidal constituents are damped more, but low frequency waves are slowed more (Parker, 1984). Amin (1985) and Pingree and Griffiths (1987) have shown that the influence of bottom

friction is such that damping is proportionally large with small amplitude constituents and small with large constituents.

In a shallow estuary, there is a frictional effect of one tidal constituent on another. Although the semi-diurnal tide M_2 with a period of 12.42 hrs greatly dominates all other constituents, such as S_2 (principal solar tide with a period of 12.0 hr) and N_2 (larger lunar elliptic tide with a period of 12.66 hr), the cumulative effect on M_2 of other constituents is significant. Therefore, model calibration should ideally include forcing from all those constituents.

However, inclusion of many constituents in the model requires long simulation times for adequate tidal analysis. The dominant tidal constituents such as M_2 , S_2 , and N_2 can be investigated in isolation using numerical models, but analysis of the M_2 tide alone provides a useful depiction of factors dominating the frictional effects. Analysis of the M_2 tide alone yields an ideal preliminary evaluation of, for example, how eelgrass distribution acts as a frictional drag on water movement.

2. Great Bay Estuary, NH

In this paper, we applied a vertically averaged, 2-D, non-linear, finite element model, ADAM (Ip *et al.*, 1998), to the Great Bay Estuary, NH (Figure 1). The Great Bay

Estuary is located in the New Hampshire seacoast region. The geomorphology of the estuary is complex. Portsmouth Harbor at the mouth of the estuary and the lower Piscataqua River can be modeled as a channel. The tidal prism in this section of the estuary is the lowest in the system, but is dominated by the tidal flow of the entire system (Short, 1992).

In considering tidal flow dynamics, the Great Bay Estuary can be divided into two sections: the Piscataqua River and the Little Bay/Great Bay section. The tidal flow down bay from the narrow channel at Dover Point is more dissipative with a progressive tidal wave character. The flow in the Little Bay/Great Bay section is less dissipative and has a standing wave character (Swift and Brown, 1983).

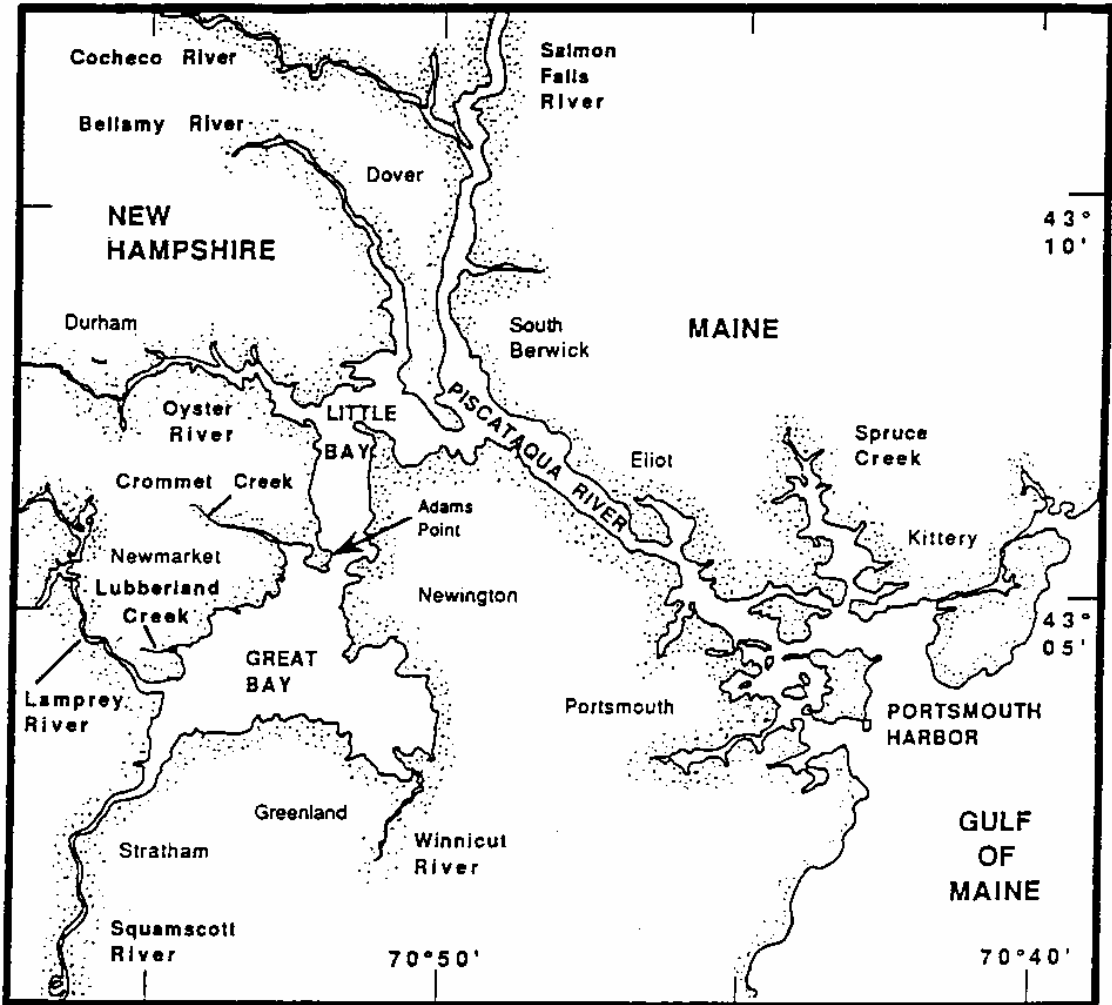


Figure 1- Great Bay Estuary, NH-ME (Short, 1992).

At the mouth of the estuary near Portsmouth the average tidal range is 2.7m decreasing to 2.0m at Dover Point, increasing slightly to 2.1m at the mouth of Squamscott River (Short, 1992). The phase of the tide lags inward from the ocean. At Dover Point, the tide is 1.3 hours behind Portsmouth Harbor, at Adams Point it is 2.25 hours later and in the Lower Squamscott River it is 2.4 hours behind (Swift and Brown, 1983). Maximum current speeds are 0.5 m/s in Little Bay/Great Bay section, and are

between 0.5 m/s and 2.0 m/s at stations in the Piscataqua River. Current speeds are inversely proportional to the channel cross-sectional area (Swift and Brown, 1983).

Little Bay is an L-shaped section of the estuary joining the Piscataqua River at Dover Point, to Great Bay at Adams Point. A deep central channel characterizes Little Bay with tidal flats on both sides. Little Bay turns sharply at Fox Point, creating complex flow patterns and a great deal of turbulence. Little Bay is dominated by tidal flow including up-bay effects from Great Bay. The Great Bay is a wide, shallow bay characterized by tidal flats, a deep main channel and a network of drainage channels. The water surface of Great Bay covers 23km² at mean high water (MHW) and 11km² at mean low water (MLW) (Short, 1992). More than 50% of the surface area of Great Bay is exposed as mud flat or eelgrass flat at low tide. River flow varies seasonally with a maximum in spring. Tides dominate over freshwater input throughout the year. Reichard and Celikkol (1978) showed that fresh water input from rivers is around 2% of the tidal prism and there is an approximate equal ground water flow (T. Ballestero, pers. com.). As the freshwater input is low in the Great Bay Estuary, tidal currents are more important than density-driven circulation (Swift and Brown, 1983).

2.1. Eelgrass Habitat in Great Bay, NH

Eelgrass, *Zostera marina*, L., is the most common temperate seagrass species. Tremendous variation in size and in the length of eelgrass blades can be found from 6cm to over 300cm long. A sheath at the base of the blade encompasses 3-5 strap-like leaves. The blades connect to the rhizome at the sediment surface with roots extending into the substrate at each rhizome node. A terminal mature shoot occurs at the end of each rhizome, with young shoots occurring as lateral branches

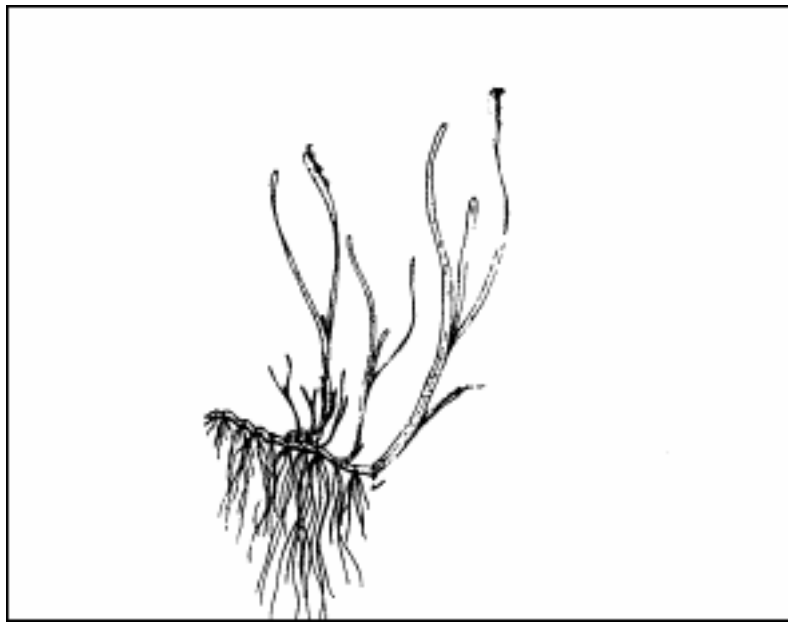


Figure 2- Eelgrass, *Zostera marina* L. (Fonseca, 1998)

Eelgrass, a submerged marine flowering plant, is rooted in the sediments of coastal and estuarine waters of the northern temperate oceans. The plants form underwater beds or meadows, and contribute significantly to the health and productivity of coastal areas (Thayer *et al.*, 1989). Eelgrass is important in the life cycle of lobsters, crabs, finfish, geese and ducks (Short, 1992). Eelgrass habitats form valuable sediment traps and help to stabilize bottom sediments (Ward *et al.*, 1984). The leaves of eelgrass

form a three-dimensional baffle in the water, acting as dampers and reducing water motion. The structure of eelgrass habitat, with floating leaves extending into the water column, altering current circulation and flow patterns, provides a mechanism for entrapment of sediments and larval organisms suspended within the water column (Grizzle *et al.*, 1996). Eelgrass meadows act as a filter of estuarine waters, removing both suspended sediments and dissolved nutrients (Short and Short, 1984).

3. Effects of Eelgrass on the Local Current Flow

The momentum extracted by exposed eelgrass shoots significantly reduces current speeds within the meadow (Short *et al.*, 1974, Harlin *et al.*, 1982, Madsen and Warncke, 1983, Peterson *et al.*, 1984 and Fonseca *et al.*, 1983). The perturbations in flow and sediment transport caused by eelgrass meadows may also significantly affect the ecology of the resident plant and animal community.

Eckman (1987) suggested that:

- Current flux through the meadow depends directly on the density of eelgrass shoots,

- Rates of recruitment of bivalves onto eelgrass blades vary directly with the shoot density dependent current flux,

- Subsequent growth rates and survival of suspension feeding bivalves vary directly with the shoot density dependent flux of seawater through the meadow.

Fonseca and Kenworthy (1987), in preliminary laboratory studies, suggest that currents affect leaf production of *Z. marina*. Current velocity, together with wave action, creates hydraulic regimes that influence seagrass and seedling distribution which in turn affects the flow field. Thus, when models of seagrass-dominated estuaries are constructed, consideration of frictional drag due to the seagrass may have a significant impact on the model's predictions.

4. ADAM model

The ADAM model is a non-linear, 2-D, depth averaged, time stepping, finite element model (Ip *et al.*, 1998). This model incorporates two-dimensional wave physics with a porous medium beneath the sediment surface to simulate flooding and dewatering processes on tidal flats on a fixed, high-resolution mesh.

The objective of this study was to investigate the friction effects of eelgrass on the tidal flow in Great Bay analyzing only the M_2 tidal constituent. The area of interest, particularly Great and Little Bays, is characterized by a network of channels with tidal flats on the sides. The primary reason for choosing the ADAM model was the importance of the flooding/dewatering process on the tidal flats. The following were also taken into account:

- The Great Bay Estuary is small enough to neglect the Coriolis accelerations, and it is vertically mixed. ADAM is a depth-integrated model, which adequately treats the dynamics in the Great Bay Estuary.

- The primary force balance is between friction and the pressure gradient in most shallow tidal embayments (Friedrichs *et al.*, 1992). Swift and Brown (1983) verified this balance observationally throughout the Great Bay Estuary. In ADAM, the acceleration terms in the momentum equation are neglected and the force balance is reduced to its simplest form, which is the balance between the bottom friction and the pressure gradient.

- The representation of the flow regime at very low water levels has been an ongoing problem in hydrodynamic modeling. In some models, the elements are entirely deactivated when they are sufficiently dry. However, this approach causes some numerical instability as the depth goes to zero. In ADAM, a heterogeneous porous medium underlying the water column is used to represent continuous, slow drainage. Flow in the porous medium is described by Darcy's law (Ergun, 1952).

- In time stepping models, the governing equations are discretized in time using a finite difference strategy. The main advantage of time stepping models is their ability to incorporate all the non-linearities. The most significant disadvantages are issues regarding proper specification of time dependent boundary conditions and forcing, the

large size of output data sets, and the computational time required (on the order of days in this case). In ADAM, the non-linear diffusion equation is discretized on linear finite elements by the Galerkin method (Burnett, 1987) in space and solved implicitly with iteration in time. The time dependent boundary conditions and forcing were easily specified. The priority was to resolve the non-linearities. In order to resolve the non-linearities, we accepted the necessity of greater computational time and storage space.

4.1. Governing Equations

In ADAM model, vertically averaged velocities are used. The continuity and the horizontal momentum equations are

$$\frac{\partial H}{\partial t} + \nabla \cdot H\bar{v} = 0 \quad (1)$$

$$\frac{\partial \bar{v}}{\partial t} + \bar{v} \cdot \nabla \bar{v} + \bar{g} \nabla \xi + \frac{C_d}{H} |\bar{v}| \bar{v} = 0 \quad (2)$$

where H is the total water column depth, ∇ is the horizontal gradient differential operator, \bar{v} is the vertically averaged horizontal current, ξ is the surface elevation relative to a horizontal datum, \bar{g} is the gravitational acceleration, C_d is the bottom friction coefficient and t is time.

As the primary balance is between the bottom friction and the pressure gradient in shallow tidal embayments, the momentum balance reduces to

$$\bar{g}\nabla\xi + \frac{C_d}{H}|\bar{v}|\bar{v} = 0 \quad (3)$$

$$\text{and} \quad \bar{v} = -\sqrt{\frac{\bar{g}\nabla\xi H}{C_d}} \quad (4)$$

Adding a porous layer beneath the sediment surface allows a natural transition, as the water level is lowered, from pure open-channel flow to a Darcian flow. To achieve this transition the variation of the porosity and conductivity of the medium is specified as a function of depth as shown in Figure 3. Because of this formulation, intertidal areas continue to participate hydraulically in the overall system, and the free surface of the water is allowed to fall below the usual bathymetric depth, providing increased stability to the model equations.

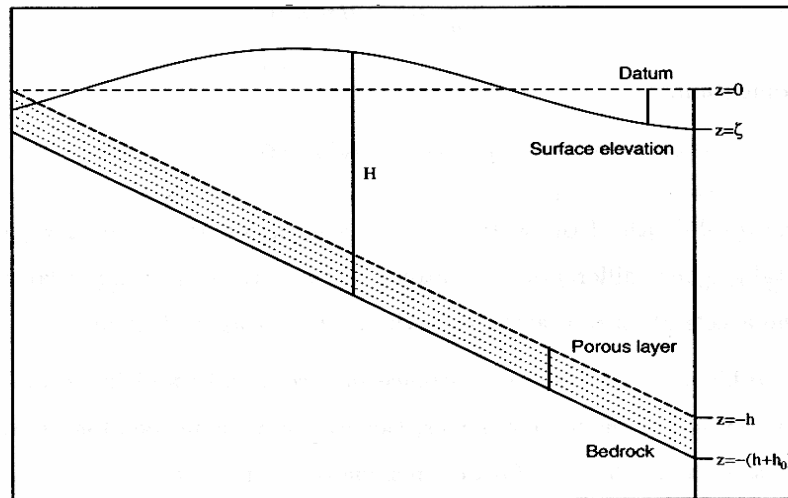


Figure 3- Porous layer beneath the sediment surface (Ip *et al.*, 1998).

The non-linear diffusion equation is discretized on linear finite elements by the Galerkin method in space and a solution is obtained iteratively in each time step.

5. Methods

The principal lunar tide, M_2 , with a period of 12.42 hours has important influences on regional currents. Therefore, our initial focus was on the M_2 harmonic constituent and its biharmonics. ADAM was tested for its ability to compute M_2 tidal dynamics in the Great Bay Estuary. The predicted M_2 tidal elevations from Swift and Brown (1983) were used in the verification of the model. Then the friction effects of eelgrass on tidal flow were explored.

5.1. Bottom Friction Coefficient

We adjusted the bottom friction coefficient for the M_2 tidal constituent until the model results fit to predicted amplitude and phase data from Swift and Brown (1983). The tidal flow, velocities and tidal heights were predicted in simulations of Great Bay with a standard bottom friction distribution and with the addition of eelgrass as a frictional drag in flow velocity calculations.

Three different bottom friction coefficient distributions were tested with M_2 tidal forcing and without any eelgrass (Fig. 4). In simulation A, a constant bottom friction coefficient, C_d , with a value of 0.005 is applied throughout the estuary. The model overpredicted both the surface elevations and the velocities with this constant bottom friction coefficient. In order to resolve the high friction in shallow areas, we let the bottom friction coefficient to linearly change with depth in simulation B. In this simulation, the model underpredicted both the surface elevations and the velocities. Thus, in simulation C, we decreased the bottom friction coefficient, keeping it depth dependent. The bottom friction coefficient distribution in simulation C, was found to be the optimum distribution. The relationship between the bottom friction coefficient and depth is given by the following equation:

$$C_d=A-B \times h$$

In simulation C, $A=1 \times 10^{-2}$ and $B=1.97 \times 10^{-4}$ [1/m] for the $0\text{m} < h < 25.4\text{m}$ depth range of M_2 tidal forcing.

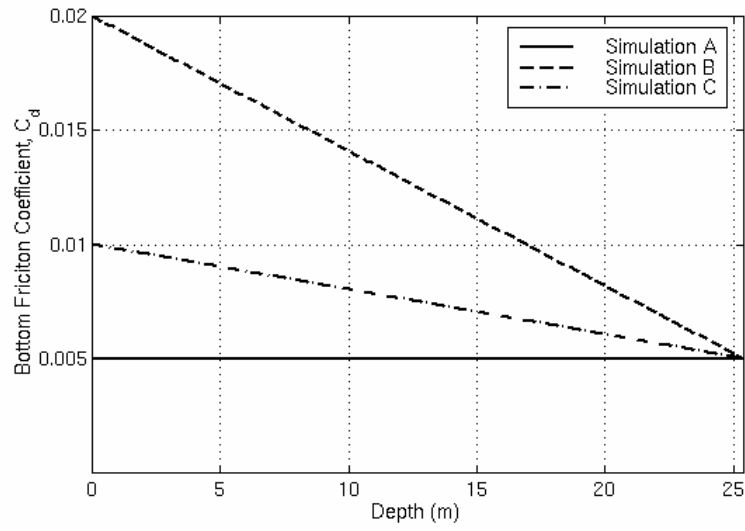


Figure 4- Bottom friction coefficient distribution for simulations A, B and C.

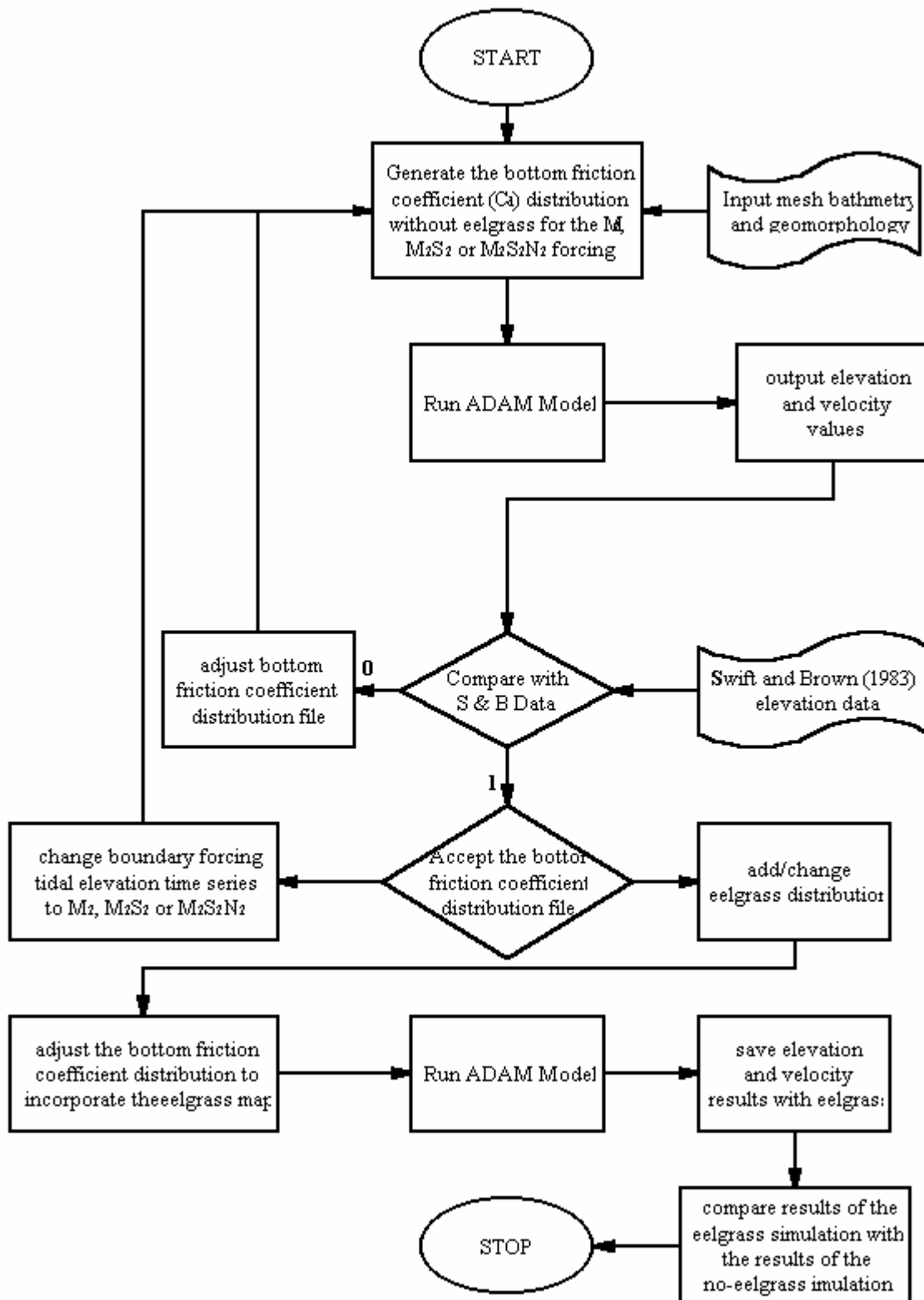


Figure 5- Flow-chart for calibration of the model.

5.2. Computational Setup and Parameters for the Entire Estuary

The Great Bay Estuary model was discretized with 39617 triangular elements and 22140 nodes. Bathymetry values were assigned at each node. Tidal forcing was applied along a transect at Portsmouth Harbor. Four hundred time steps were used per tidal cycle. The simulations were started with fluid at rest and were terminated after six M_2 tidal cycles when dynamic equilibrium was reached. In order to handle the dewatering process on the tidal flats in Great Bay, a heterogeneous porous medium underlying the water column was used. Porous layer thickness was assigned a 1m depth, approximately one third of the M_2 tidal range in Great Bay. For porosity (ϵ), 0.35 was used which is between the porosity value for sand ($\epsilon=0.25$) and clay ($\epsilon=0.50$). The hydraulic conductivity in this layer was set to 3.162×10^{-4} throughout the estuary. The simulation parameters are presented in Table 1.

Table 1- Simulation parameters for the ADAM model.

Bathymetry range	$0 \leq h \leq 25.40\text{m}$
Porous layer thickness	$h_0 = 1.00\text{m}$
Hydraulic conductivity	$k = 0.0003162$
Bottom friction coefficient	See Figure 4
Time increment	$\Delta t = 111.78 \text{ sec}$
Time steps per tidal period	400
Tidal periodicity	$T = 12.42 \text{ hr.}$
Length of simulation	6T

Numerical implicity	$\theta = 1$
Number of non-linear iterations	4

5.3. Comparison Methods for the Entire Estuary

The surface elevation time series produced by the model were compared to the surface elevation time series (reference data) predicted by the tidal analysis of Swift and Brown (1983) at tidal stations Seavey, T-11, T-12, T-13, T-14A, T-14, T-16, T-UNH, and T-19 (see Figure 6). The cross-section averaged velocity time series produced by the model was compared with the reference velocity time series at stations C-104, C-119, C-124 and C-131.

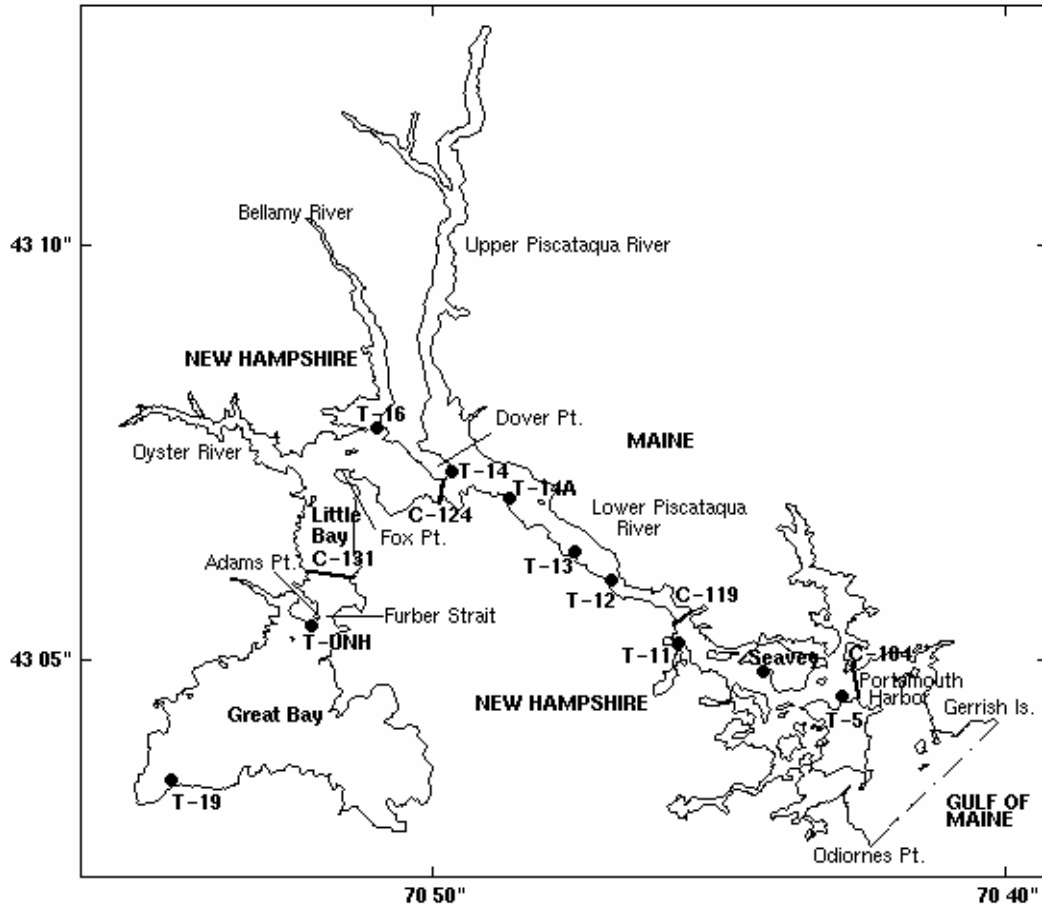


Figure 6- Stations for reference data in Great Bay Estuary where tidal surface elevations (T) and current velocity cross sections (C) were monitored in 1975 (Swift and Brown, 1983).

The correlation coefficient is a measure of the strength of the relationship between the model output and the reference data (Bendat and Piersol, 1986). The correlation coefficient (*Cor*) is calculated as follows:

$$Cor(\text{model, reference}) = \frac{C(\text{model, reference})}{\sqrt{C(\text{model, model})C(\text{reference, reference})}}$$

where C is the covariance matrix.

The Root Mean Square error is a measure of the deviation of the model output value from the reference value (Bendat and Piersol, 1986). The Root Mean Square is used to quantitatively measure how closely the model output variable tracks the reference data. The magnitude of the Root Mean Square error is evaluated by comparing it to the mean of the time series:

$$RMS_N = \frac{\sqrt{\text{mean}(\text{model} - \text{reference})^2}}{\text{std}(\text{reference})} \quad \text{where std is the standard deviation.}$$

5.4. Computational Setup and Parameters for Great Bay

To resolve a surface elevation phase problem between the model output and the reference data at stations T-UNH and T-19, the mesh was cut at Little Bay and a new tidal forcing boundary was applied. The new boundary forcing was obtained by interpolating tidal analysis predictions from the reference data set at various stations in the estuary.

In this simulation of Great Bay only, the number of nodes in the mesh was reduced from 22140 to 5657 and the number of elements was reduced from 39617 to 10526. Number of time steps per tidal cycle was reduced from 400 to 300. Changes in the mesh size and time step reduced the computing time by 83%. In the new mesh, the

maximum element area was 8389m^2 and the minimum element area was 40m^2 . Parameters changed from the entire estuary simulation were bathymetry range (0 - 18.5 m), time increment ($\Delta t = 149.047$ sec), and the time steps per tidal period (300).

6. Results

6.1. M_2 Tidal Flow without Eelgrass in the Entire Great Bay Estuary

Elevation results compare well with the reference data (see Figure 7) up the estuary to station T-16. The model underpredicts the amplitudes up estuary from station T-16 with a visible phase difference.

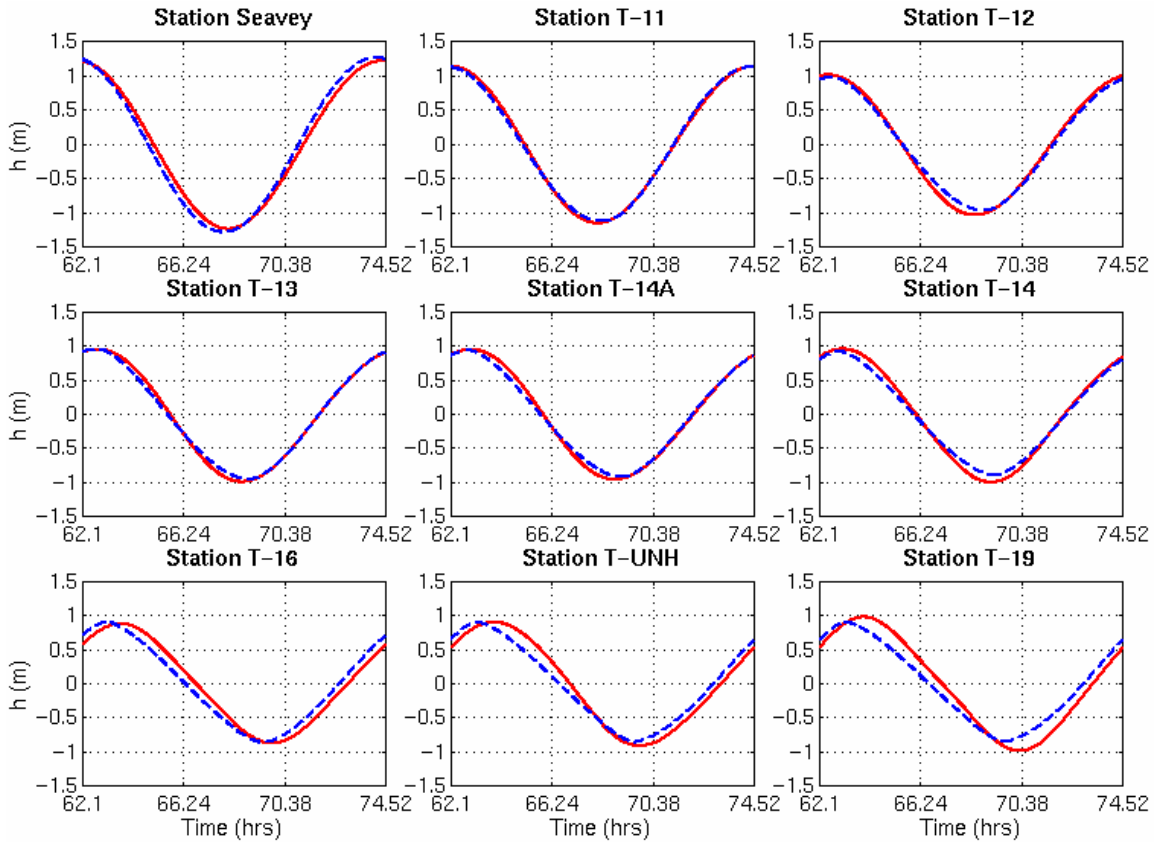


Figure 7- Surface elevation comparisons of model outputs with tidal analysis reference data. Solid lines indicate reference data and dashed lines indicate model-produced data.

The comparison of cross-section averaged velocity values (see Figure 8) shows that the model overpredicts the velocities at all stations.

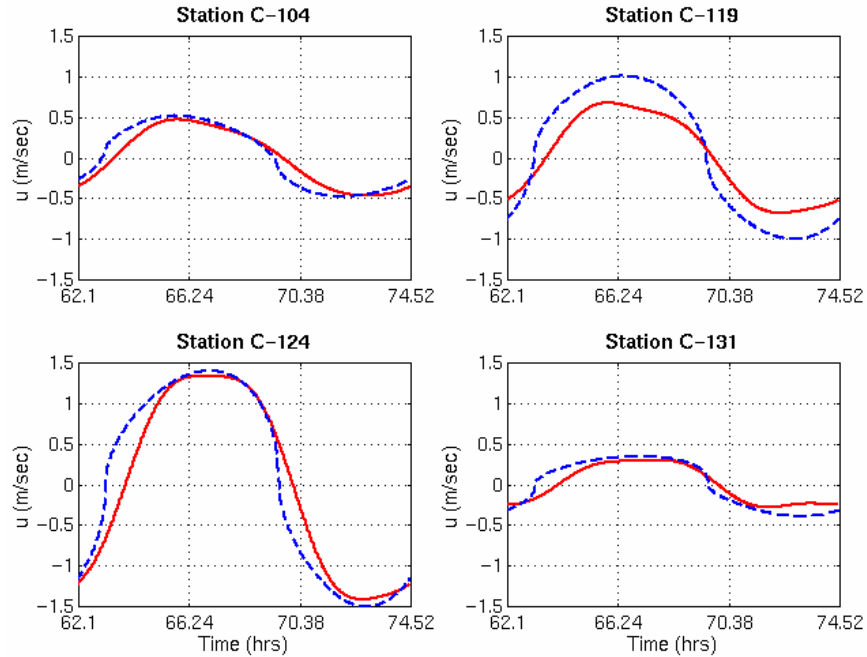


Figure 8- Comparison of cross-section averaged velocity values with tidal analysis reference data. Solid lines indicate reference data and dashed lines indicate model-produced data.

6.2. M_2 Tidal Flow without Eelgrass in Great Bay Section

At specified stations, the model results are compared with the tidal analysis predicted time series. The comparison of surface elevation and cross-section averaged velocity values at stations T-UNH, T-19 and C-131 show improved agreement (Figures 7, 8 & 9) and the statistical analyses of those comparisons confirm the improved simulation results.

The model produced surface elevation time series at stations T-UNH and T-19 compare well to the tidal analysis reference data, with 8% and 12% RMS error,

respectively. The RMS error between the model produced cross-section averaged velocity time series and the tidal analysis reference data at station C-131 is 31%.

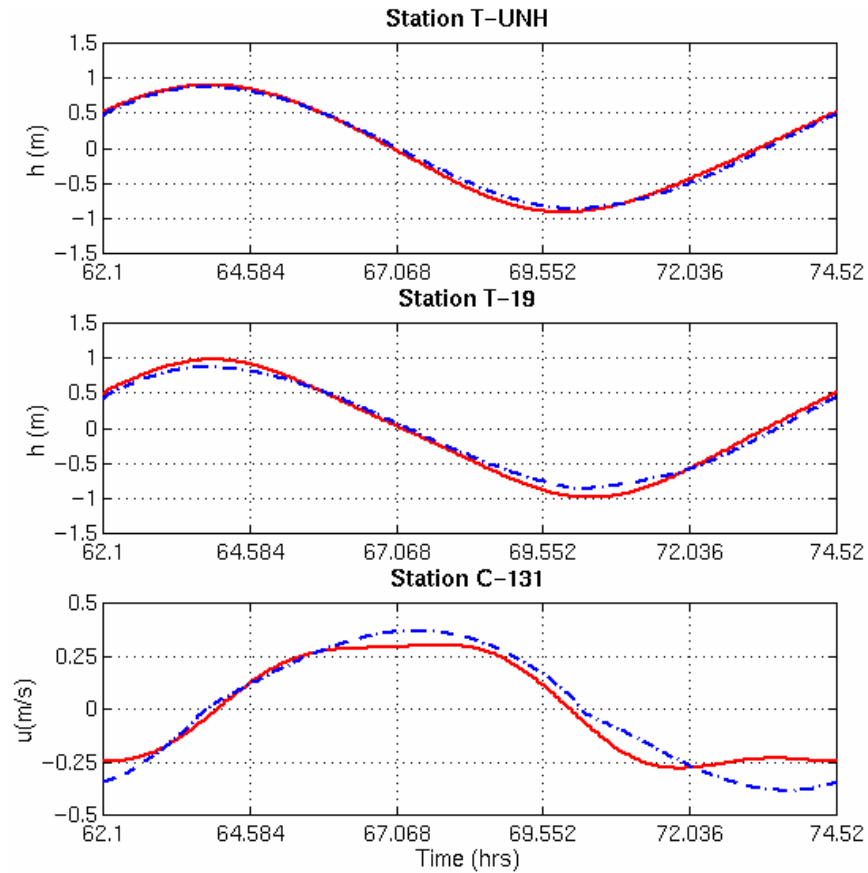


Figure 9- Comparison of model produced times series (solid lines) and tidal analysis reference data (dashed lines) at stations T-UNH, T-19 and C-131. Top figure shows the comparison of surface elevation at station T-UNH. The middle figure shows the comparison of surface elevation at station T-19. The bottom figure shows the comparison of cross-section averaged velocity at station C-131.

6.3. Eelgrass Effects on the M_2 Tidal Flow in Great Bay

The water surface of Great Bay covers 19.02km² at mean high water and 10.63km² at mean low water. The model calculated average depth is 2.62m at mean high water and 1.97m at mean low water. Based on this fact, the model predicts that 44% of the surface area in Great Bay drains at low M₂ tides when no eelgrass is included in the model.

Eelgrass beds are treated as extra dampers to water flow in the model. The bottom friction coefficient distribution found for M₂ tidal forcing without eelgrass (Figure 4) is used with an adjustment at nodes where eelgrass beds exist (Figure 10). The bottom friction coefficient within eelgrass beds is adjusted to 0.1 (Kopp, 1999). The difference in water velocity magnitudes and directions was analyzed with and without eelgrass for twenty-seven stations in Great Bay (Figure 10).

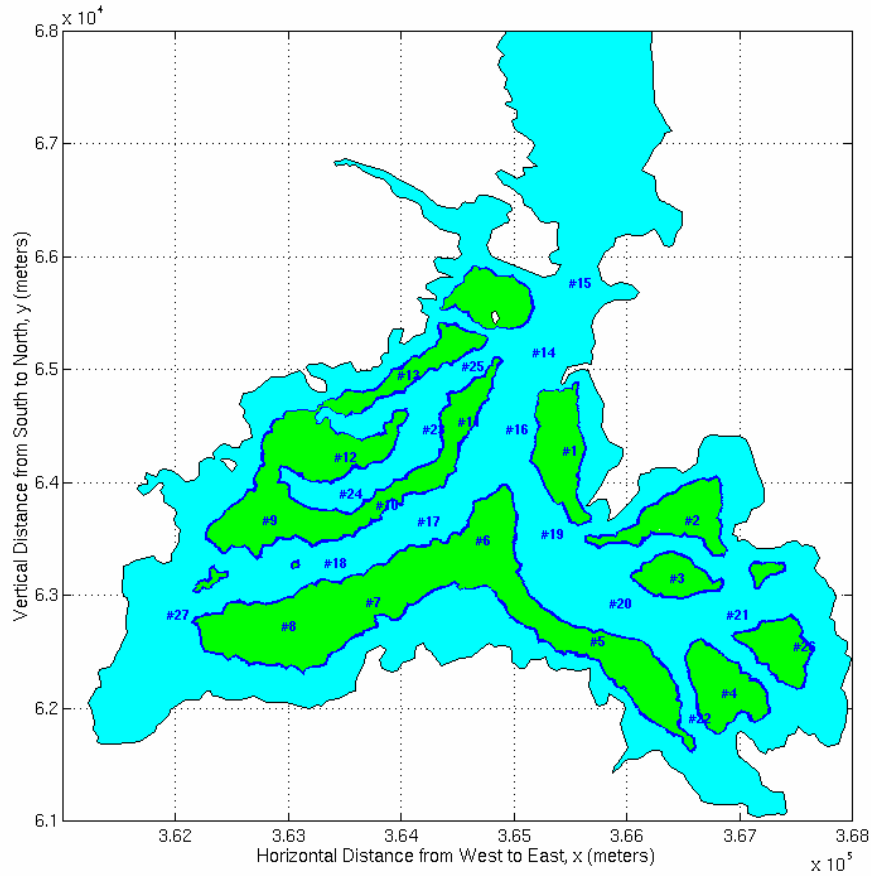


Figure 10- Map of eelgrass distribution in Great Bay, 1990. Eelgrass is shown in green, with the selected stations numbered from 1-27 for sampling hydrodynamic results from the model.

The addition of eelgrass to the ADAM model of Great Bay changes the surface area and the average depth at mean low water, but does not have any effect on these elements at mean high water. With eelgrass incorporated in ADAM, the low tide surface area of Great Bay increases to 12.20km^2 . The low tide surface area with eelgrass is 1.57km^2 larger than the surface area at mean low water without eelgrass. These results show that, due to the high friction values, eelgrass holds water on the tidal flats at low tide, keeping a greater surface area wet.

Addition of eelgrass to the model alters the tidal flow, forcing the flow to channelize into deep areas, increasing the velocities in the deep channels and decreasing the velocities over the eelgrass beds. Changes in the magnitude and direction of current velocities at selected stations in Great Bay with and without eelgrass show distinct differences (Figures 11-13). Inclusion of eelgrass in the model decreases current speeds at stations, which are over eelgrass beds (stations 1 through 13, and station 26, Figures 10, 11a-c). Station 15 is in the deep channel and far away from eelgrass; no significant effect of including eelgrass in the model is observed at this station (Figure 11b). At all other stations, which are in the channels between the eelgrass beds, current velocities increase due to eelgrass effects (Figures 11a-c).

At all stations over the eelgrass beds, the currents change direction compared to the non-eelgrass simulation. That is, with eelgrass in the model, currents tend to flow more directly toward the nearest channel rather than in the overall direction of tidal flow. In the tidal channels, no significant change in the current direction is observed whether or not eelgrass is included in the model. Depending on the position of a station in relation to eelgrass beds (Figure 10), a systematic change in velocity (speed and direction) can be identified with stations in the middle of an eelgrass bed showing changes a wider range of directions and dramatically reduced speeds (stations 1 - 4, 6 - 9). Stations at the edge of an eelgrass bed (stations 5, 10-13) show a relatively consistent shift in direction with substantial reduction in speed. In contrast, stations within the tidal channels away from the eelgrass beds (stations 14, 16-21, 25, 27) generally show a small (to no) shift in

direction accompanying an increase in speed as more water flows through the tidal channels.

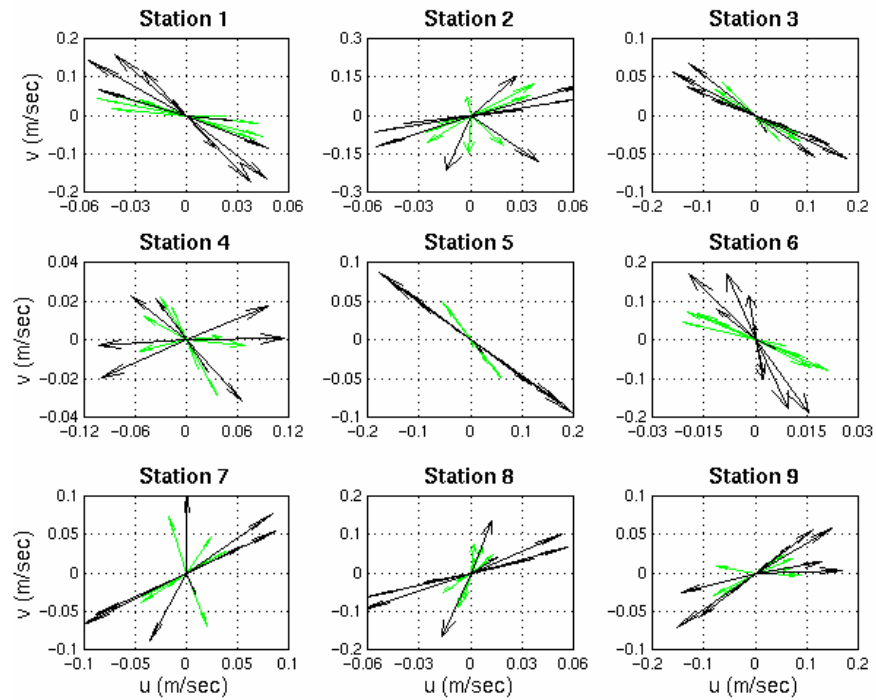


Figure 11-a.

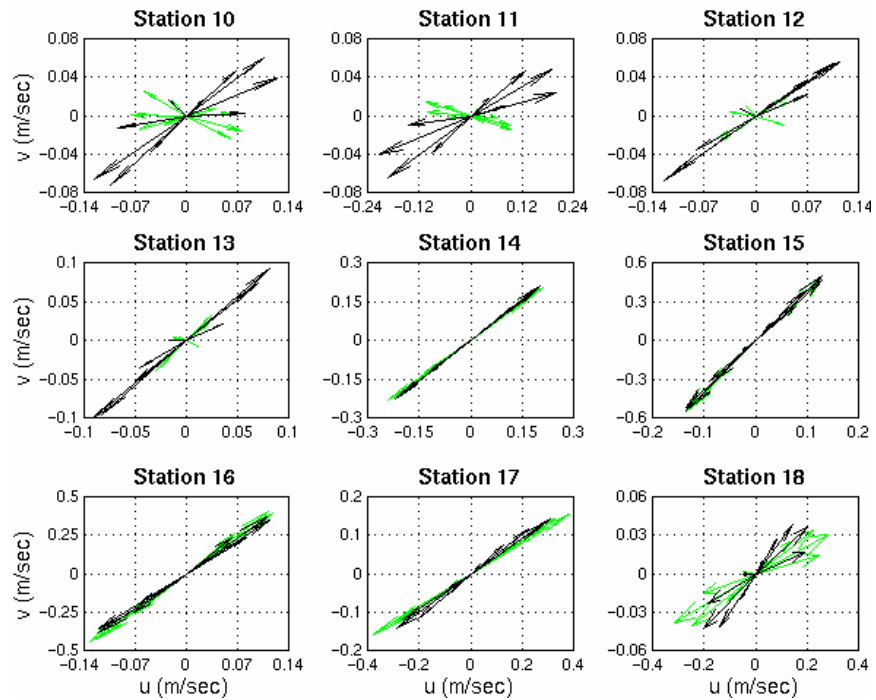


Figure 11-b.

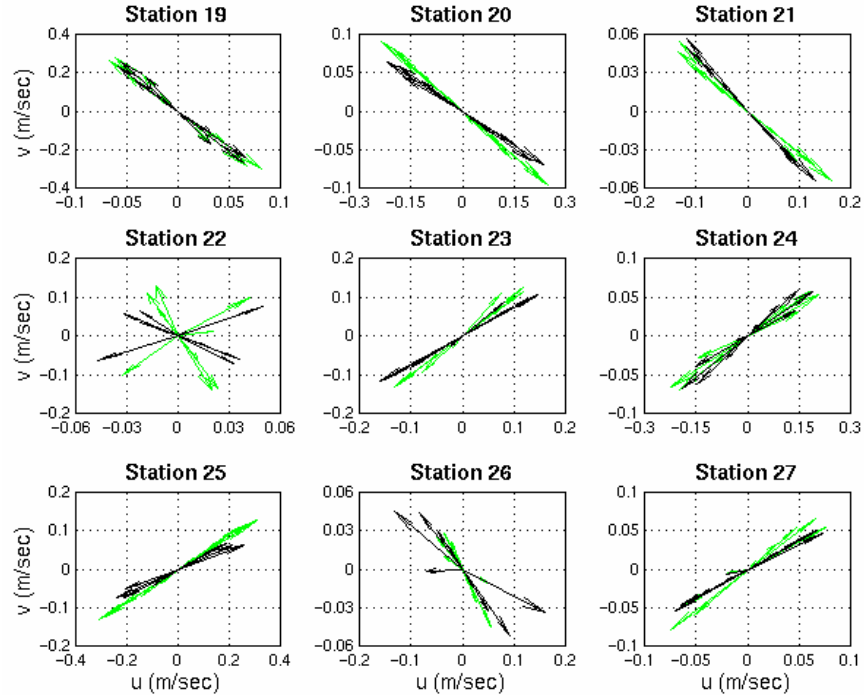


Figure 11-c. Model simulation of Great Bay, NH, with M_2 forcing, showing magnitude and direction of velocity vectors over one tidal cycle. Comparison of model-produced velocity values with (green) and without (black) eelgrass distribution at stations 1-9 (a), stations 10-18 (b), and stations 19-27 (c).

Current speeds reach their highest values at maximum ebb and flood tidal stages. To examine the impact of eelgrass, we plotted the highest velocities achieved at each node with and without the plant's presence (Figures 12-14). The maximum velocities observed in Great Bay occur in Furber Strait, where the cross-sectional area of the channel is smallest. The highest predicted velocity value in the Furber Strait is 1.29m/s for the ebb stage and 1.35m/s for the flood stage. The velocities decrease to 0.4m/s - 0.5 m/s in the channels in southeast and southwest Great Bay. The velocity distribution on the tidal channel and flat at maximum ebb in the east Great Bay with and without eelgrass shows that presence of eelgrass slowed down the current flow over the tidal flats (Figure 12). Also, a visible change in the direction of the flow over the tidal flats is

observed. On the other hand, the velocities are increased in the deep channel next to the tidal flat.

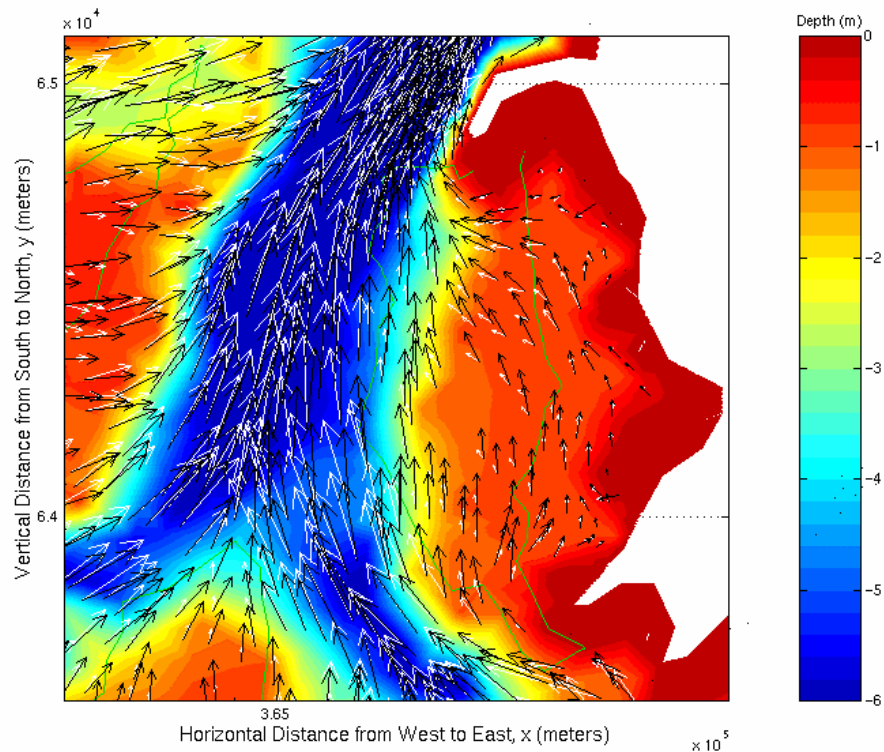


Figure 12- Model simulation of east Great Bay, NH, with M_2 forcing, showing magnitude and direction of velocity vectors for maximum ebb current at each node, displayed over a bathymetry map. Velocities without eelgrass distribution are shown with black vectors. White vectors indicate the velocities with eelgrass. Eelgrass beds are surrounded by a green contour.

In south Great Bay, there are tidal channels on the east and west side of the eelgrass flat (Figure 13). The velocity values on the flat over the eelgrass bed decrease due to the friction effects of eelgrass. The velocity vectors over the tidal flats on the eelgrass bed are directed towards the tidal flat outside the eelgrass bed. On the other hand, the velocities in the channels increase with a slight change in direction when eelgrass is included in the simulation.

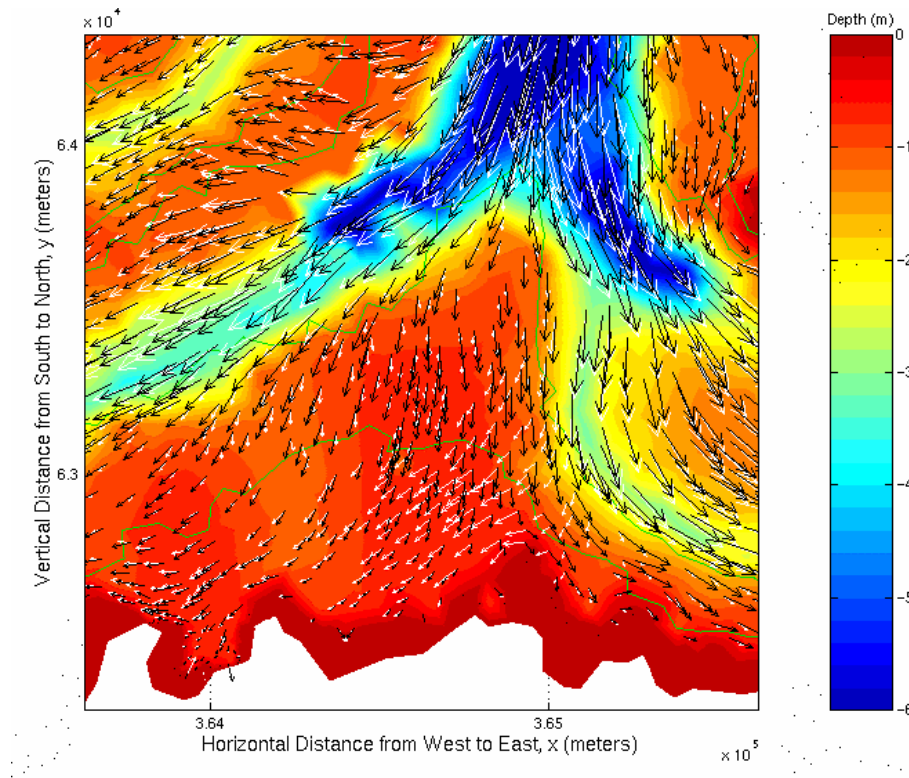


Figure 13- Model simulation of south Great Bay, NH, with M_2 forcing, showing magnitude and direction of velocity vectors for maximum flood current at each node, displayed over a bathymetry map. Velocities without eelgrass distribution are shown with black vectors. White vectors indicate the velocities with eelgrass. Eelgrass beds are surrounded by a green contour.

In southwestern Great Bay (Figure 14), the velocity vectors on the tidal flat outside the eelgrass bed are directed around the eelgrass bed towards the deep channel in west and an almost 90° change in current direction (compared to the no-eelgrass simulation) is observed outside the eelgrass beds. The model indicates that water flows preferentially around the eelgrass bed rather than across the bed.

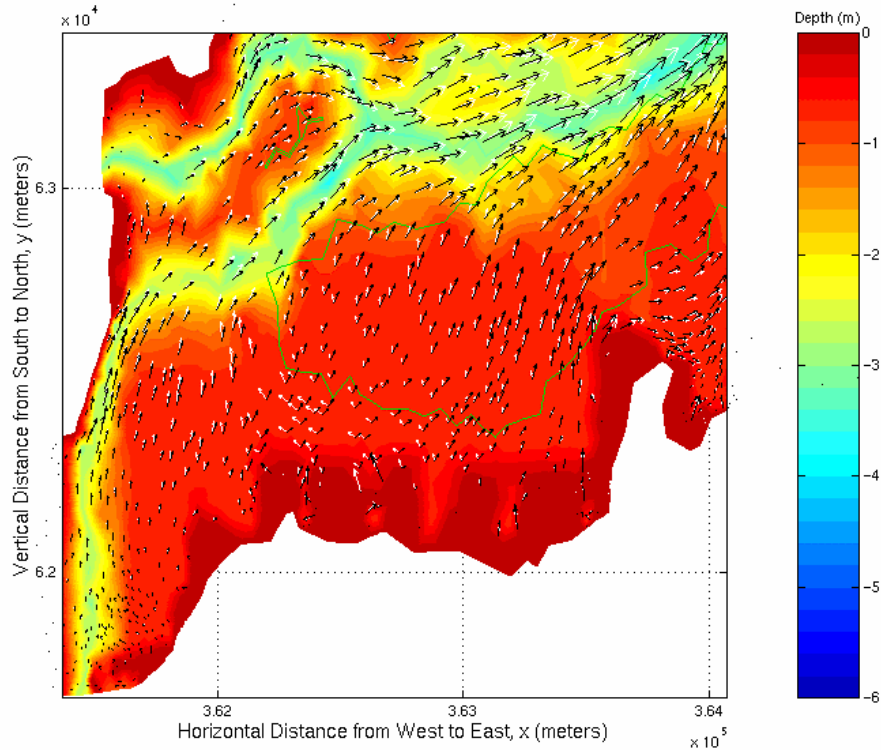


Figure 14- Model simulation of southwest Great Bay, NH, with M_2 forcing, showing magnitude and direction of velocity vectors for maximum ebb current at each node, displayed over a bathymetry map. Velocities without eelgrass distribution are shown with black vectors. White vectors indicate the velocities with eelgrass. Eelgrass beds are surrounded by a green contour.

7. Conclusions and Discussion

We investigated the effectiveness of the ADAM model in simulating tidal flow in Great Bay with flooding and draining on the tidal flats. Simulation of the flow field in Great Bay with the ADAM model was comparable to the available reference data. The Great Bay is characterized by a network of channels with tidal flats on the sides. The model results show that 44% of Great Bay is exposed as tidal flats at mean low water with M_2 tidal forcing. A transition from ebb dominance in the channels to flood

dominance in the shallow tidal flats, which is the real dynamics in that section, is obtained with ADAM model simulations.

The ADAM model was calibrated for the M_2 tidal forcing by adjusting the bottom friction coefficient and the bottom friction coefficient values were modified to reflect eelgrass distribution in 1990. Eelgrass beds were treated as extra dampers and the friction coefficients were increased to reflect the presence of eelgrass.

The frictional effects of eelgrass distribution on the tidal flow in Great Bay were explored. Addition of eelgrass to the model:

- alters the velocity within eelgrass beds
- alters the velocity in the channels
- increases the water surface area at mean low water
- changes the direction of current patterns within the estuary.

Modeling the eelgrass effects on the tidal flow by increasing the bottom friction is a good approximation and gave physically realistic results. Currents have significant effects on the eelgrass growth (Eckman, 1987). The current patterns found in this study are going to be used in predicting potential eelgrass mitigation areas in Great Bay and they are going to serve as input data for a biological model.

In future, other significant tidal contributors, such as S_2 and N_2 tidal components are going to be added to the simulations in order to resolve the spring-neap cycles in Great Bay.

Acknowledgements

This study was supported by the Cooperative Institute for Coastal and Estuarine Environmental Technology, CICEET, (grant # NA 87OR0512). We would like to thank Dr. D.R. Lynch and Dr. J.T. Ip, who generously shared their finite element code with us. We would like to thank Dr. B. Çelikkol for supporting this research and Dr. A. Bilgili for exchanging valuable information. We would like to thank C.A. Short and graduate student C. Burdick for their help in editing the manuscript.

References

- Amin, M., 1985. Temporal Variations of Tides on the West Coast of Great Britain. *Geophysical Journal of Royal Astronomical Society*, 82, pp.179-199.
- Bendat, J.S., Piersol, A.G., 1986. *Random Data Analysis and Measurement Procedures*, John Wiley and Sons, NY.
- Burnett, D.S., 1987. *Finite Element Analysis from Concepts to Applications*, Addison-Wesley Publishing Company, pp.53-54.
- Celikkol, B., Reichard, R., 1976. *Hydrodynamic Model of The Great Bay Estuarine System*, Technical Report UNH-SG-153, pp.1.
- Eckman, J.E., 1987. The Role of Hydrodynamics in Recruitment, Growth, and Survival of *Argopecten irradians* (L.) and *Anomia simplex* (D'Orbigny) within Eelgrass Meadows. *Journal of Experimental Marine Biology and Ecology*, 106, pp.165-191.
- Ergun, S., 1952. Fluid Flow Through Packed Columns. *Chem. Eng. Progr.*, 48(2), pp. 89-94.
- Fonseca, M.S., Zieman, J.C., Thayer, G.W., Fisher, J.S., 1983. The Role of Current Velocity in Structuring Eelgrass (*Zostera marina* L.) Meadows. *Estuarine Coastal Shelf Science*, 17, pp. 367-380.
- Fonseca, M.S., Kenworthy, W.J., 1987. Effects of Current on Photosynthesis and Distribution of Sea Grasses. *Aquatic Botany*, 27, pp. 59-78.

Friedrichs, C.T., Lynch, D.R., Aubrey, D.G., 1992. Velocity Assymetries in Frictionally-Dominated Tidal Embayments: Longitudinal and Lateral Variability. In: Prandle, D. (Ed.), *Dynamics and Exchnages in estuaries and the Coastal Zone, Coastal and Estuarine Studies*, 40, American Geophysical Union: Washington D.C., pp. 277-312.

Grizzle, R.E, Short, F.T., Newell, C.R., Hoven, H., Kindblom, L., 1996. Hydrodynamically Induced Synchronous Waving of Seagrasses: 'Monami' and its Possible Effects on Larval Mussel Settlement. *Journal of Experimental Marine Biology and Ecology*, 206, pp.165-177.

Harlin, M.M., Thorne-Miller, B., Boothroyd, J.C., 1982. Seagrass-Sediment Dynamics of a Flood-Tidal Delta in Rhode Island (U.S.A). *Aquatic Botany*, 14, pp.1108-1116.

Ip, J.T.C., Lynch, D.R., Friedrichs, C.T., 1998. Simulation of estuarine Flooding and Dewatering with Application to Great Bay, New Hampshire. *Estuarine Coastal and Shelf Science*, 47, pp. 119-141.

Kopp, B.S., 1999. Effects of Nitrate Fertilization and Shading on Physiological and Biomechanical Properties of Eelgrass (*Zostera marina* L.). PhD. Thesis, University of Rhode Island.

Kreiss, H., 1957. Some Remarks About Non-linear Oscillations in Tidal Channels. *Tellus*, 9, pp. 53-68.

Madsen, T.V., Warncke, E., 1983. Velocities of Currents around and within Submerged Aquatic Vegetation. *Arch. Hydrobiology*, 97, pp. 389-394.

Parker, B.B., 1984. *Frictional Effects on the Tidal Dynamics of a Shallow Estuary*, Ph.D. Dissertation, Johns Hopkins University, Baltimore, Maryland.

Peterson, C.H., Summerson, H.C., Duncan, P.B., 1984. The Influence of Seagrass Cover on Population Structure and Individual Growth Rate of a Suspension Feeding Bivalve, *Mercenaria mercenaria*. *J. Marine Research*, 42, pp.123-138.

Pingree, R.D., Griffiths, D.K., 1987. Tidal Friction for Semidiurnal Tides. *Continental Shelf Research*, 7, pp. 1181-1209.

Pritchard, D.W., 1955. *Estuarine Circulation Patterns*, Proc. ASCE, 81(717).

Short, F.T., 1992. *The Ecology of The Great Bay Estuary, NH and ME: An Estuarine Profile and Bibliography*. Jackson Estuarine Laboratory, UNH, Durham, NH.

Short, F.T., 1987. Effects of Sediment Nutrients on Seagrasses: Literature Review and Mesocosm Experiments. *Aquatic Botany*, 27, pp.42-57.

Short, F.T., Short, C.A., 1984. The seagrass filter: Purification of Estuarine and Coastal Waters. In: Kennedy, V.S. (Ed.), *The Estuary as a Filter*. Academic Press, pp.395-413.

Short, F.T., Nixon, S.W., Oviatt, C.A., 1974. Field studies and simulation with a fine grid hydrodynamic model - seagrass and circulation in Charlestown Pond. In: *An Environmental Study of a Nuclear Power Plant at Charlestown, R.I.*, University of Rhode Island 33, VI-B, pp. 1-27.

Swift, M.R., Brown, W.S., 1983. Distribution of Bottom Stress and Tidal Energy Dissipation in a Well-Mixed Estuary. *Estuarine Coastal and Shelf Science*, 17, pp. 297-317.

Ward, L.G., Kemp, W.M., Boynton, W.R., 1984. The influence of waves and seagrass communities on suspended particulates in an estuarine embayment. *Mar Geol.*, 59, pp.85-103.